

# Aptamer C10.36 Reveals a Ribonucleoprotein Complex on the Surface of Non-Hodgkin Lymphoma Cells Providing Candidates for Multi-Target Therapeutics

Sonal S. Tonapi<sup>1</sup>, Janet E. Duncan<sup>1</sup>, Vaishali Pannu<sup>1</sup>, Matthew Rosenow<sup>1</sup>, Qing Zhang<sup>1</sup>, Melissa Richards<sup>1</sup>, Teresa L. Tinder<sup>1</sup>, Heather A. O'Neill<sup>1</sup>, Mark R. Miglarese<sup>1</sup>, David Spetzler<sup>1</sup>, Michael Famulok<sup>1,2,3</sup> and Günter Mayer<sup>1,2</sup>

<sup>1</sup>Caris Life Sciences, Phoenix, AZ, USA; <sup>2</sup>LIMES Program Unit Chemical Biology & Medicinal Chemistry, University of Bonn, Bonn, Germany; <sup>3</sup>Chemical Biology Max-Planck-Fellowship Group, Center of Advanced European Studies and Research (CAESAR), Bonn, Germany



## Abstract

**Introduction:** Aptamers are valuable tools for identifying novel therapeutic targets due to their high affinity and specificity. The relative ease of selection of aptamers binding to complex targets and their lack of immunogenicity have led to the incorporation of aptamers into drug transport vehicles and cell labeling tools. However, their potential as direct anti-cancer therapies remains to be explored. Recent advances in aptamer therapeutics have underscored their potential to meet the need for better therapies in B-cell non-Hodgkin lymphomas (NHL). For example, the aptamer AS1411 binds nucleolin and inhibits the proliferation of multiple leukemia and lymphoma cancer cell lines. The DNA aptamer C10.36 has been shown to selectively bind to Ramos Burkitt lymphoma cells and to be internalized via clathrin-dependent endocytosis. Here we identify the molecular target of C10.36 and explore its potential role as a targeted therapy in NHL.

**Results:** C10.36 affinity pull-downs revealed that it associates with a ribonucleoprotein complex on the surface of Ramos cells. Gene Ontology enrichment analysis revealed proteins over-represented in chromatin organization and RNA metabolic process gene sets. Covalent crosslinking identified heterogeneous nuclear ribonucleoprotein U (hnRNP U) as a direct binding target of C10.36 within the complex. We next surveyed additional lymphoma and leukemia cell lines for C10.36 binding. Interestingly, C10.36 binding to MEC-1 and SU-DHL-1 cells was readily observed, whereas binding to normal B cell derivative, SKW6.4, was greatly reduced. Although hnRNP U was detected on the surface of all four cell lines by cell surface protein labeling, affinity purification of hnRNP U by C10.36 was only observed in the fully transformed cell lines and not in SKW6.4 cells. This observation indicates that C10.36 binding may be determined by conformation, context or post-translational modification. Treatment with C10.36 led to a loss of viability and IC50 values for sensitive cell lines ranged from 100 to 400 nM. Importantly, a single point mutation in C10.36 (G24A) abrogated both binding and anti-proliferative activity.

**Conclusion:** The present study identifies cell surface hnRNP U and its ribonucleoprotein interaction partners as potential therapeutic targets for NHL and highlights the potential for the development of C10.36 as a novel anti-B cell lymphoma targeted therapy.

## Results

### C10.36 specifically binds to Ramos cells

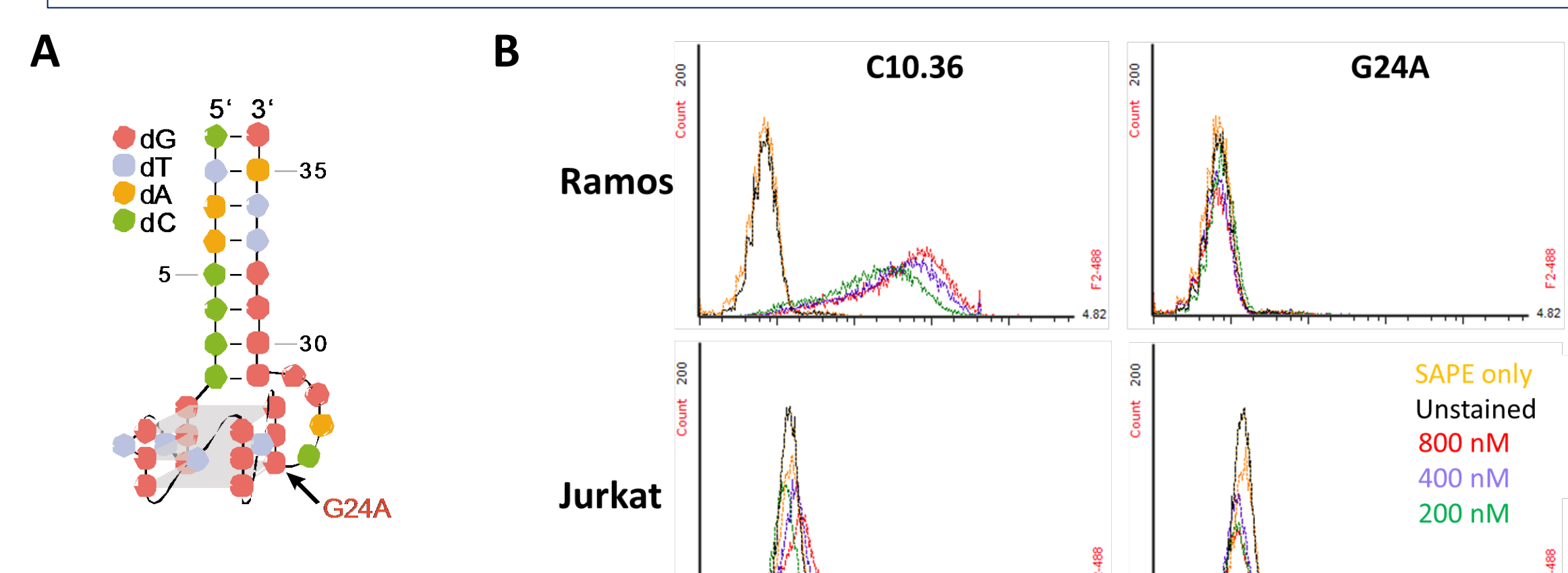


**Figure 1:** A. Proposed G-quadruplex structure of C10.36. The arrow indicates a point mutation of C10.36 within the G-quadruplex, named G24A, which results in loss of binding. B. Flow cytometry analysis of C10.36 shows specific binding to Ramos cells but not to Jurkat cells.

### Affinity purification of a ribonucleoprotein complex with C10.36

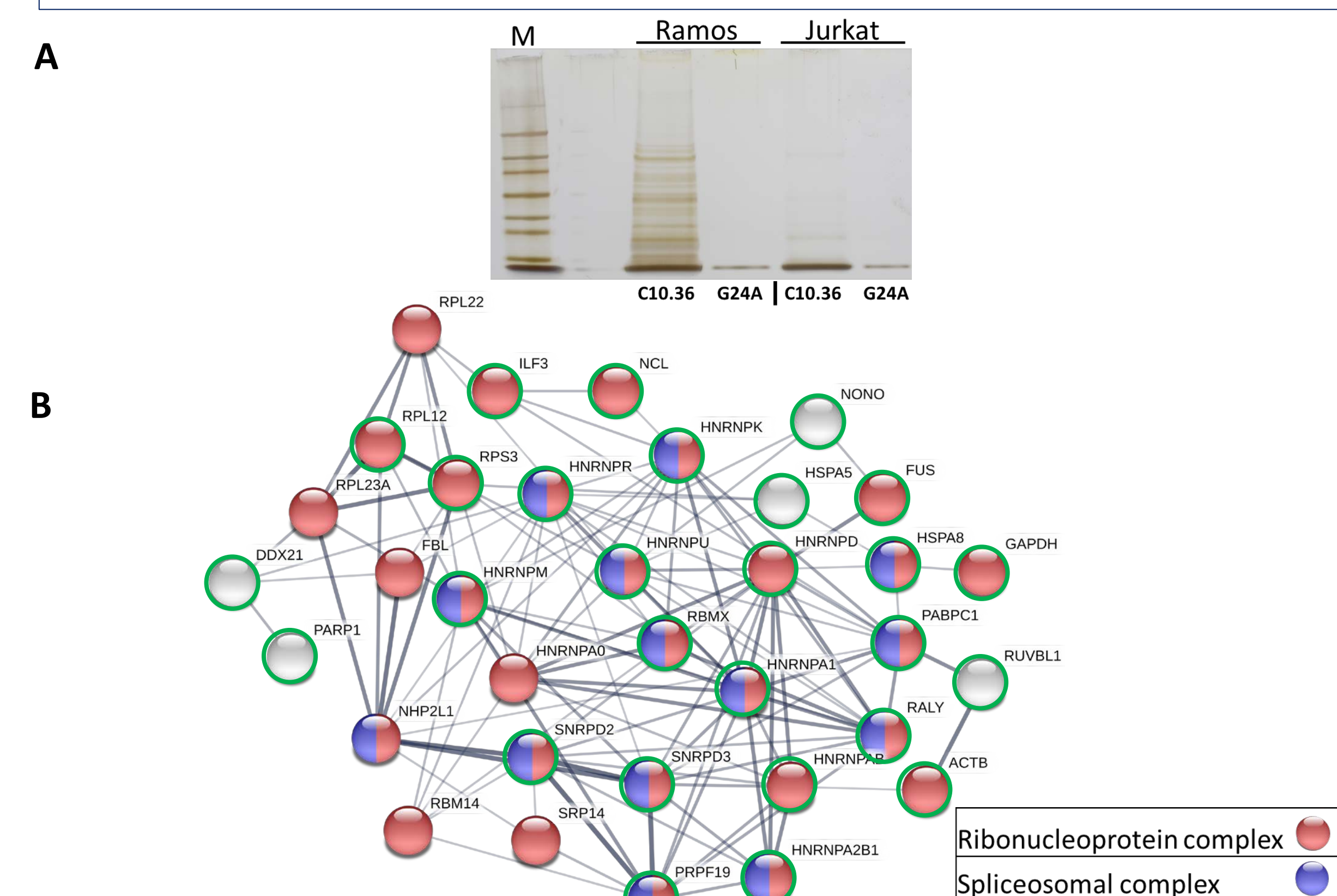


**Figure 2:** A. Affinity-purification with C10.36 shows greater number of proteins bound to C10.36 in Ramos compared to Jurkat cells. B. STRING<sup>2</sup> interaction network map of affinity purified targets unique to C10.36 with Ramos cells identifies ribonucleoprotein splicing complexes on the surface of Ramos cells. Targets circled in green were confirmed to be on the cell surface with biotin surface labeling independent of aptamer binding.

### C10.36 directly binds ribonuclear protein hnRNP U on the surface of Ramos cells

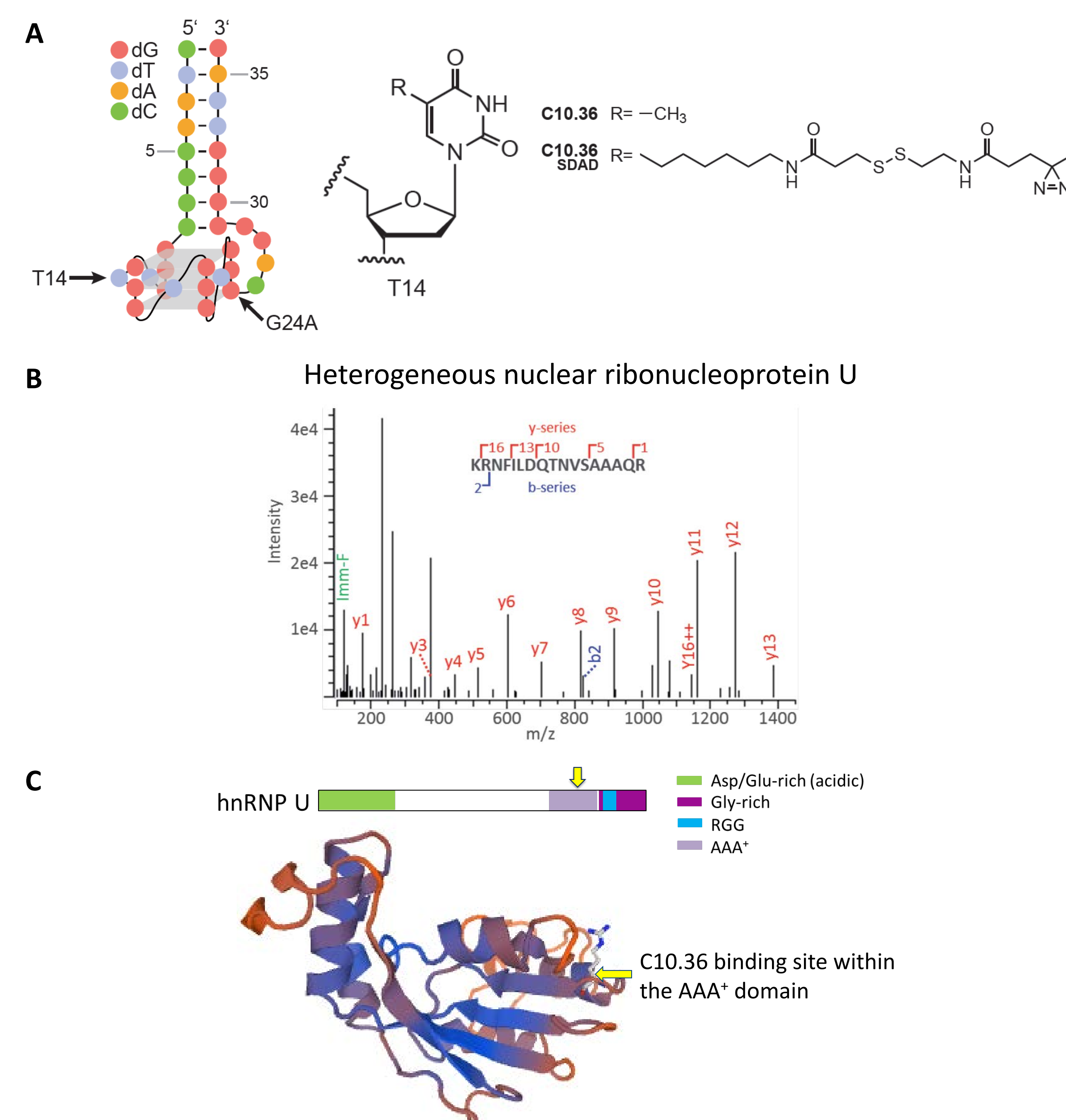


**Figure 3:** A. The direct molecular target of C10.36 was identified by label transfer from Biotin-C10.36-T14(SDAD) (shown above) to target proteins after photo-crosslinking, subsequent affinity purification and identification by LC-MS/MS. B. hnRNP U was the only protein detected with the precursor mass of the peptide with the SDAD label in the MS/MS spectrum. C. Schematic of the hnRNP U protein. Crosslinked peptide identified (indicated by the yellow arrow) above is located within the AAA\* ATPase domain which is upstream of the RNA/DNA binding RGG domain. Predicted ribbon diagram of SAF-A, modeled on PDB-3ZVL, showing putative C10.36 binding site

### C10.36 is internalized into Ramos cells by lipid raft mediated endocytosis

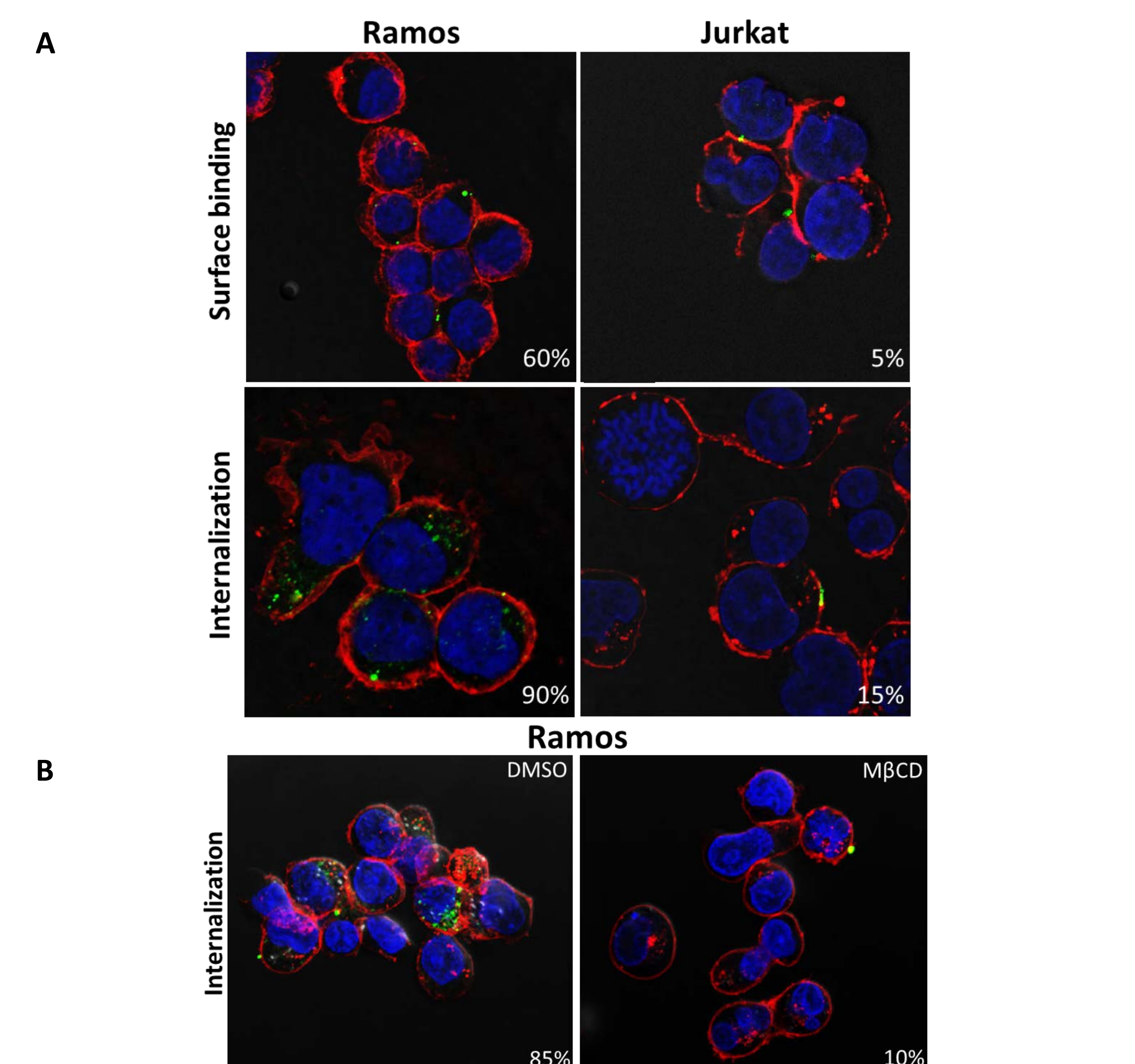


**Figure 4:** A. C10.36 internalization was assessed by confocal microscopy. C10.36 (green) was incubated with Ramos cells at 4 °C (surface binding) or 37 °C (internalization). Ramos cells specifically internalized C10.36. G24A did not show significant surface binding or internalization in either cell line (not shown). Cell membrane is stained with wheat germ agglutinin (red) and the nucleus with DAPI (blue). B. C10.36 internalization is dependent on lipid rafts. Methyl-β-cyclodextrin (MBCD) mediated removal of membrane cholesterol inhibits C10.36 uptake.

### C10.36 internalization leads to changes in splicing in Ramos cells

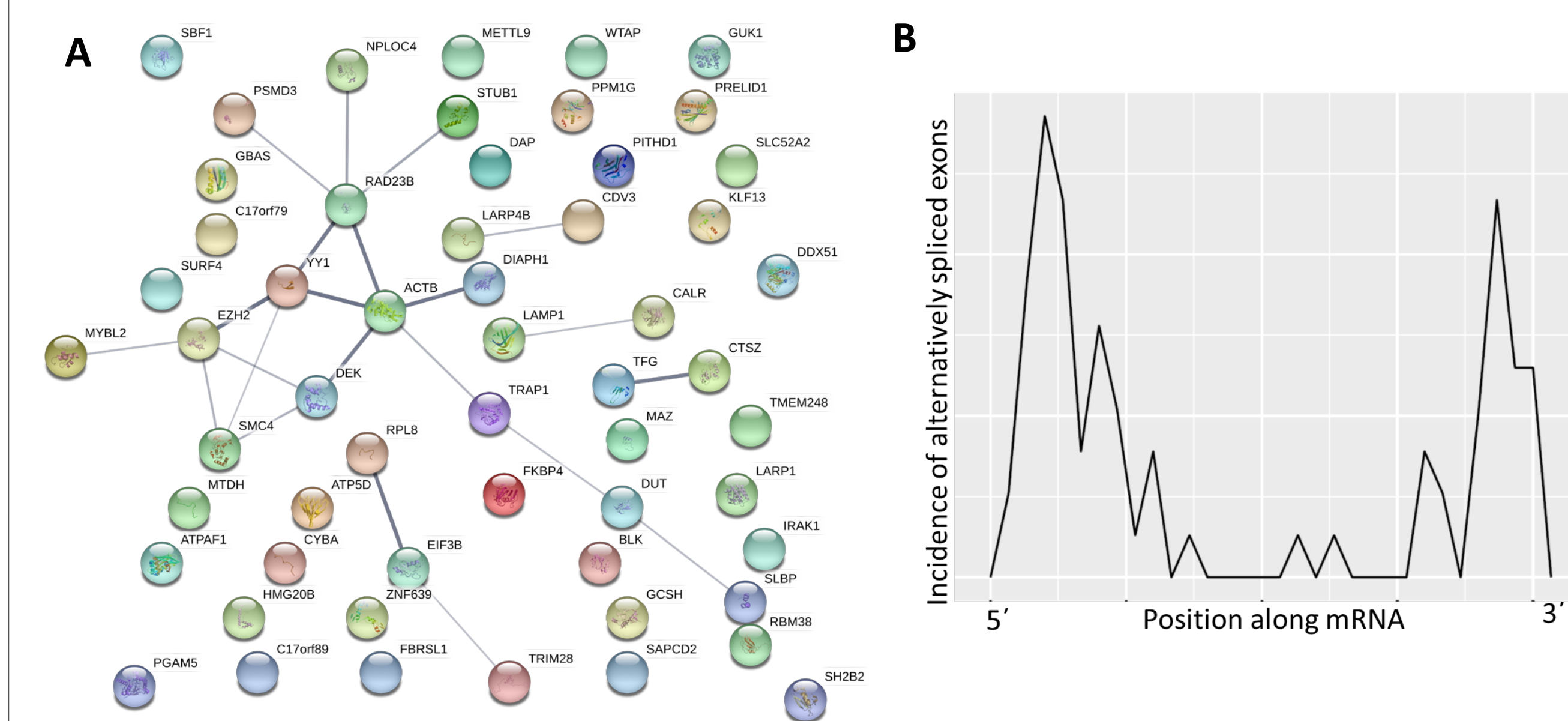


**Figure 5:** C10.36 treatment leads to alternative splicing at 24 hours. A. Alternative splicing was examined following mRNA sequencing and analysis using DEXseq. STRING network map of alternatively spliced genes indicates global impact on splicing regulation following C10.36 binding and internalization. B. The majority of the alternatively spliced exons were located in the 5' and 3' terminals of genes indicating differential usage of alternative polyadenylation (APA) sites following C10.36 treatment<sup>3</sup>.

### C10.36 treatment inhibits proliferation of Ramos cells

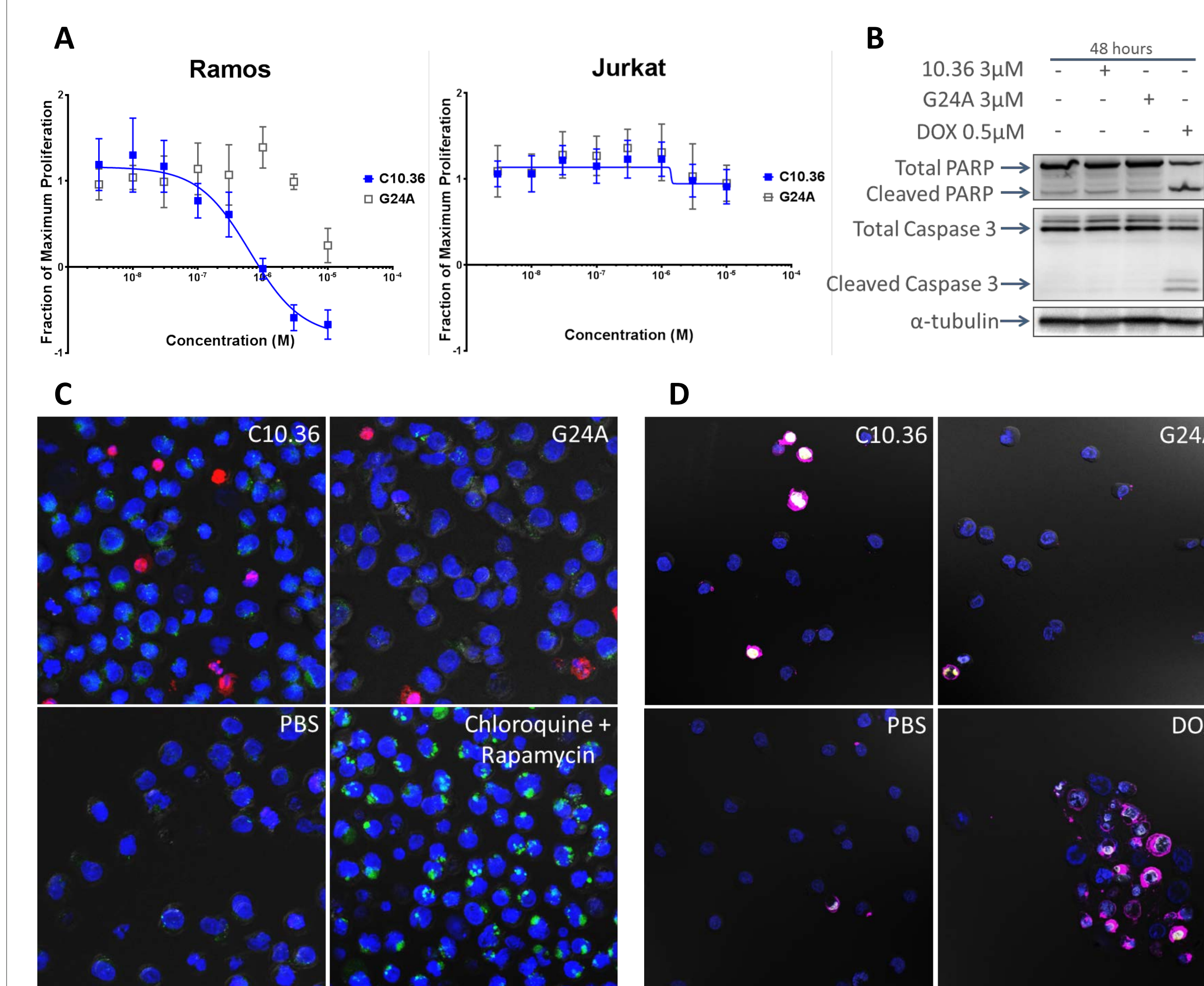


**Figure 6:** A. C10.36 inhibits proliferation of Ramos ( $IC_{50} \sim 238$ nM) cells but not Jurkat cells. Aptamers were added directly to log phase cultures and viability was assessed after 72hrs with CellTiter-Glo<sup>®</sup>. C10.36 mediated loss in viability is most likely due to necrosis as evidenced by caspase-independent cell death (B), lack of accumulation of autophagic markers (C) and positive staining with both Annexin V and SYTOX simultaneously (D). Aptamer (red) LysoTracker dye (green), Annexin V (Pink) and SYTOX (yellow).

### C10.36 decreases viability of specific non-Hodgkin lymphoma cells

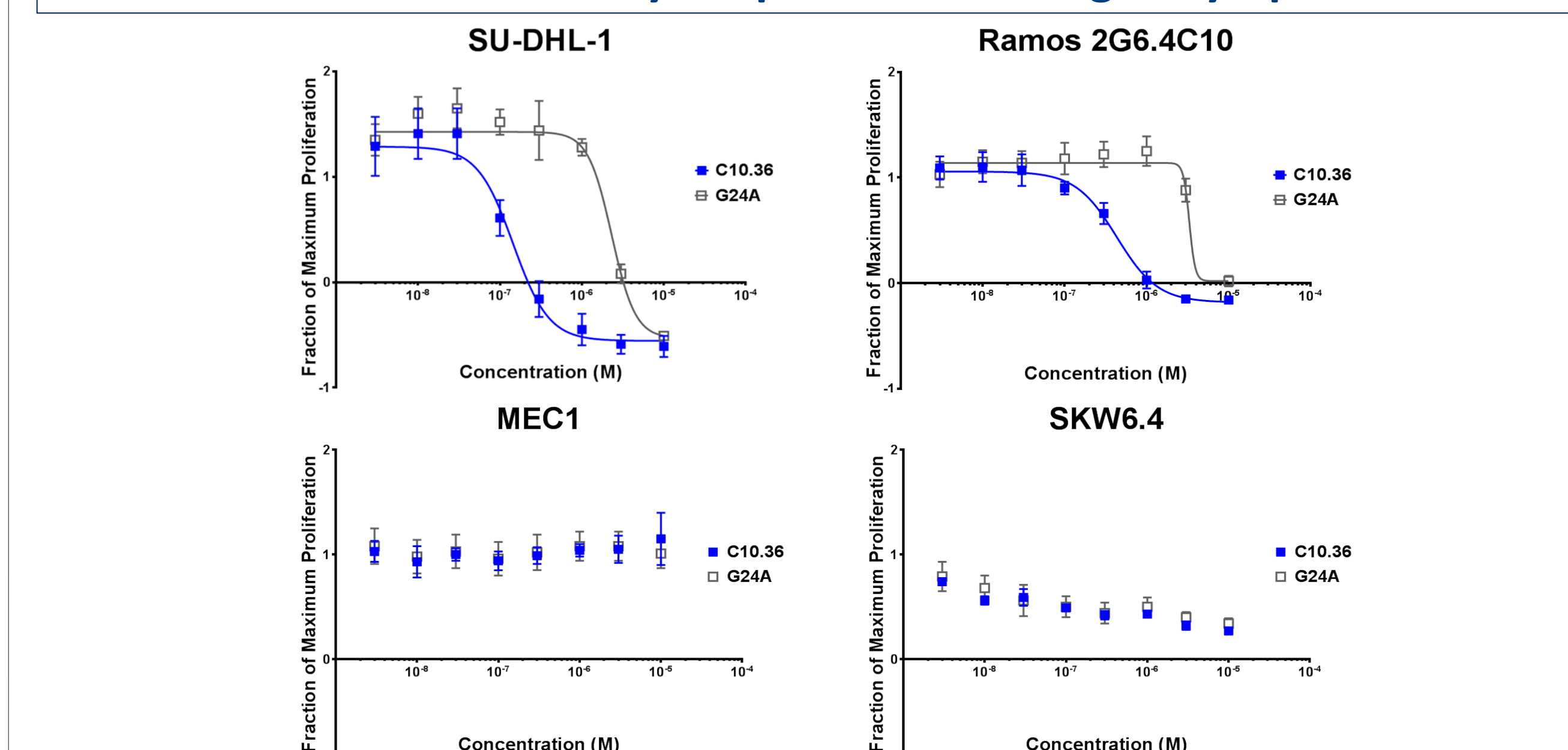


**Figure 7:** C10.36 inhibits proliferation of SU-DHL-1 ( $IC_{50} \sim 100$ nM) and Ramos 2G6.4 C10 ( $IC_{50} \sim 355$ nM) cells in a concentration dependent manner. No loss in viability was seen in MEC1 and SKW6.4, a non-tumor derived EBV transformed cell line. G24A treatment does not result in a concentration dependent decrease in viability in any of the cell lines.

### C10.36 binding and internalization are necessary for cell death

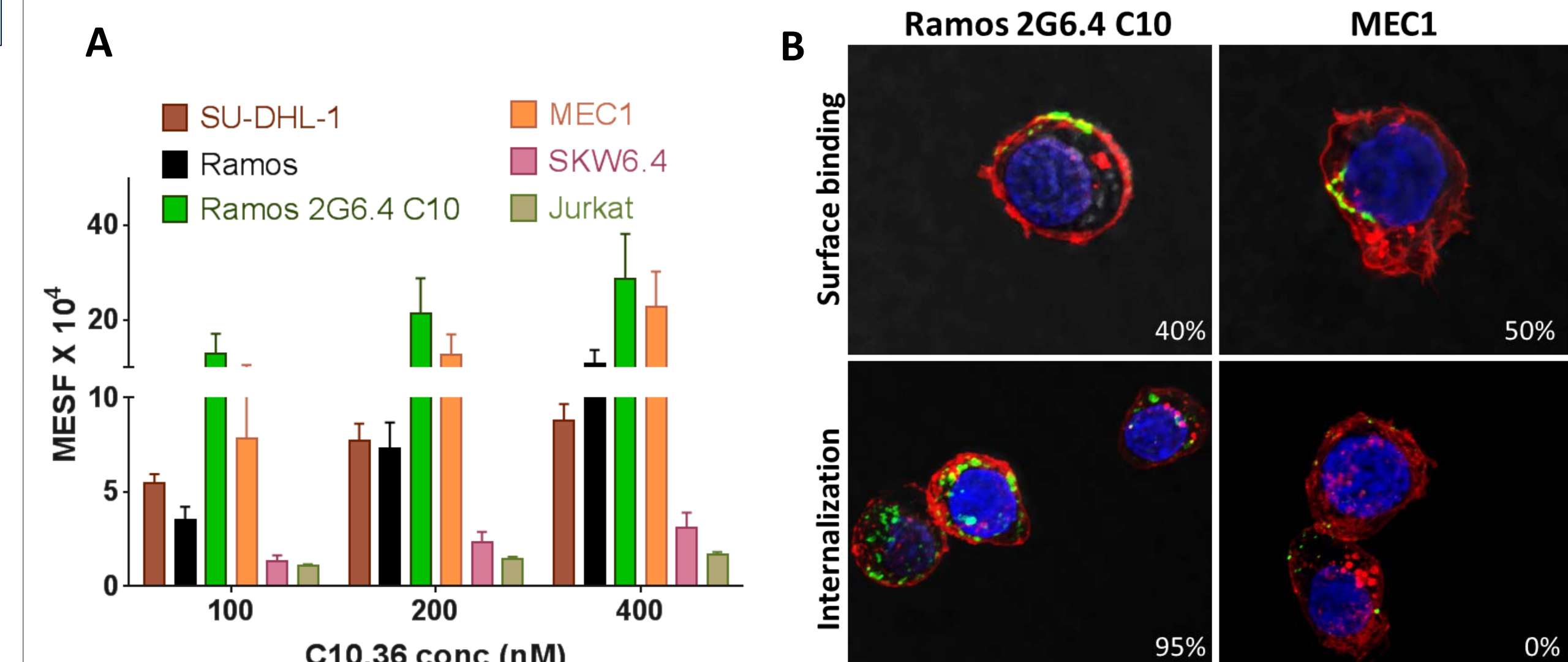


**Figure 8:** A. Preferential binding of C10.36 to different NHL cell lines was assessed by flow cytometry. Ramos 2G6.4 C10 and MEC1 cells showed highest level of binding, followed by SU-DHL-1 and Ramos cells. SKW6.4 cells displayed low binding levels, similar to Jurkat cells. B. Although MEC1 cells show greater binding to C10.36, they are not sensitive to the aptamer. Therefore we tested if MEC1 cells internalize C10.36 upon binding. Unlike the sensitive Ramos 2G6.4 C10 which internalize the aptamer (green), MEC1 cells do not. The above results indicate that binding and internalization are both required for sensitivity to C10.36. Cell membrane is stained with wheat germ agglutinin (red) and the nucleus is stained with DAPI (blue).

### Model for C10.36 mediated toxicity in non-Hodgkin lymphoma cells

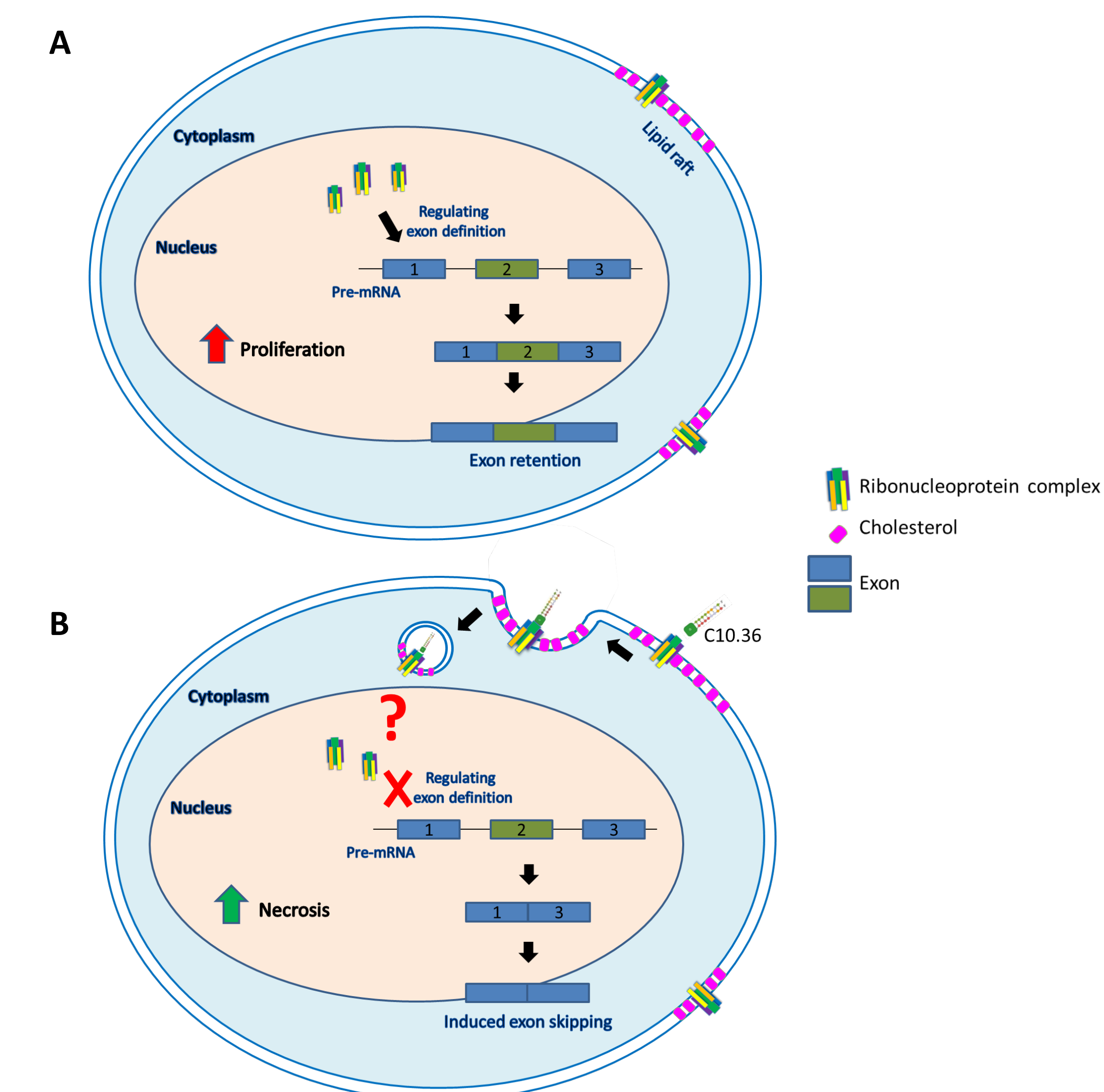


**Figure 9:** A. Ribonucleoproteins like hnRNP U are known to regulate of global splicing<sup>4</sup> in the nucleus. In NHL cells hnRNP U is also aberrantly localized in a cell surface ribonucleoprotein complex (CSRC). B. C10.36 binding to the CSRC leads to its lipid raft dependent internalization. Upon hnRNP U mediated C10.36 uptake, significant changes in splicing occur. MYC driven lymphomas are susceptible to splicing defects<sup>5,6</sup>, therefore C10.36 mediated global alternative splicing disrupts cellular homeostasis and leads to cell death by necrosis.

## Conclusions and Outlook

- The current study identifies the presence of a spliceosome complex on the cell surface of B-cell lymphomas and highlights the impact of its intracellular translocation on alternative splicing and cellular homeostasis
- As spliceosomal proteins and complexes emerge as targets of anti-cancer drugs, C10.36 represents a unique splicing targeting compound, with potential therapeutic applications

## References

- Opazo F, et al. (2015). Modular Assembly of Cell-targeting Devices Based on an Uncommon G-quadruplex Aptamer Molecular Therapy. Nucleic Acids
- Szklarczyk et al. Nucleic Acids Res. 2015 43(Database issue):D447-52
- Elkon R, et al. (2013). Alternative cleavage and polyadenylation: extent, regulation and function. Nat Rev Genet
- Xiao R, et al. (2012). Nuclear Matrix Factor hnRNP U/SAF-A Exerts a Global Control of Alternative Splicing by Regulating U2 snRNP Maturation. Mol Cell.
- Kon CM, et al. (2015). MYC regulates the core pre-mRNA splicing machinery as an essential step in lymphomagenesis. Nature
- Hsu TYT, et al (2015). The spliceosome is a therapeutic vulnerability in MYC-driven cancer. Nature

**Disclosures:** Tonapi, Duncan, Pannu, Rosenow, Zhang, Richards, Tinder, O'Neill, Miglarese, Spetzler: Caris Life Sciences: Employment. Famulok, Mayer: Caris Life Sciences: Consultancy.